Pergamon

Solar Energy, Vol. 54, No. 6, pp. 397–402, 1995

0038-092X/95 $9.50 + .00

0038-092X(95)00017-8

COSINE RESPONSE CHARACTERISTICS OF SOME RADIOMETRIC AND PHOTOMETRIC SENSORS

J. J. MICHALSKY, L. C. HARRISON, and W. E. BERKHEISER, III
Atmospheric Sciences Research Center, University at Albany,
State University of New York, 100 Fuller Rd, Albany, NY 12205 USA

Abstract—Global and diffuse irradiance and illuminance are measured with instruments that are assumed to have true cosine responses. From one refereed paper, some institutional reports, and by word-of-mouth, it is generally known that no instrument is perfect in this regard. This paper reports on measurements of cosine responses for several commercial instruments and on the cosine response of a multi-filter rotating shadowband radiometer. The measurements were made with an automated cosine response test bench using the same protocol for each instrument. The cosine bench measures with variable angular resolution as fine as 0.25°. The automated rotation is in one plane. A manual rotation allows measurements at other azimuths.

1. INTRODUCTION

The most frequently measured parameter in solar radiation research is the global (often called total) irradiance or its photometric equivalent, the global illuminance. To make these measurements, an instrument with a field of view that accepts radiation from any direction within a hemisphere is used. The assumption made when employing these devices is that the response of the instrument decreases exactly as the cosine of the angle of incidence. Figure 1 illustrates this geometry. An instrument that has this cosine response is known as a Lambertian receiver.

It is generally recognized that global irradiance and illuminance sensors do not have perfect cosine responses. It is also acknowledged that the response is poorest at the highest angles of incidence. This is most often caused by specular reflection from either the detector or the diffuser above the detector as one nears grazing incidence. The argument is often made that the cosine response is good at the highest solar elevations, i.e., the smallest angles of incidence; that most of the irradiation received is at these angles; and that the lowest elevations do not contribute enough to affect daily totals in irradiation or illumination appreciably. This is often a practical and acceptable argument.

However, there are instances when knowing the cosine response is crucial. In lieu of tracking pyrheliometer measurements, direct normal irradiance may be calculated from the simultaneous measurements of global and diffuse horizontal irradiances. The diffuse is measured with a shadowing band and corrected for blocked sky radiation. Differencing the two measurements yields the direct horizontal, from which direct normal can be calculated by dividing by the cosine of the angle between the zenith and the solar direction. Aside from the other contributions to the error that one encounters in global and diffuse horizontal irradiance measurements, the direct horizontal and, therefore, the direct normal irradiance is under or overestimated by the difference between actual and true cosine response. Tracking plates or focusing systems, for example, will not have their expected performance based on direct solar radiation measured in this fashion.

A report by Riches *et al.* (1982) contains numerous examples of measured cosine responses for several types of pyranometers still in use today. The plots in that report corroborate the earlier remarks that pyranometers do not have perfect cosine responses and that the cosine response is generally poorest at the largest angles of incidence. Individual instruments of a certain model type tend to have similar cosine responses, but differ sufficiently in that a generic cosine response is not appropriate if one is striving for maximum accuracy.

Nast (1983) made careful measurements of cosine response for every 10° of incidence angle for most of the same pyranometers tested in Riches *et al.* (1982). His study shows averaged results from several pyranometers of each type, therefore, it is difficult to assess the variability within an instrument model. Philipona *et al.* (1993) report on a sophisticated laboratory test facility that includes cosine response measurements, although isolated cosine response measurements are not included in their study.

This article reports on measurements made with an automated cosine response test bench. The measurements are made with much higher angular resolution than used in previous reports. The measurements are automated and do not require manual repositioning for each angle of incidence. The sensor position and light detection are controlled by a microprocessor-based data acquisition system used in a multi-filter rotating shadowband radiometer (MFRSR), but positioning can be controlled by any stepper motor controller. Up to three sensors of each type are measured to illustrate reproducibility within a sensor design. Although the cosine bench was actually constructed to aid in the development of MFRSRs (Harrison *et al.*, 1994), this study includes several commercial instruments that are commonly used in solar resource assessment. The next section describes the cosine response test bench. Section 3 includes results of tests of five commercial sensors. Section 4 discusses

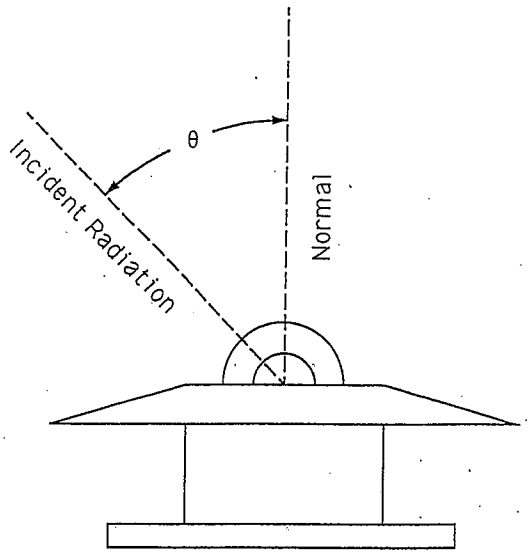

Fig. 1. This geometry defines angle of incident radiation with respect to normal for a typical 2π sr field of view sensor.

the MFRSR cosine tests, and Section 5 summarizes these results.

2. COSINE TEST BENCH

Figure 2 is a schematic layout of the cosine response test bench. The rotating table is a Daedal Model 10001. The stage is normally rotated by hand using a knurled handle. In the present application the handle is removed and the shaft on which the handle is normally mounted is coupled to the axis of a stepping motor via a custom-machined plastic coupler. The shafts, which have different diameters, are aligned and the plastic coupler is fixed to each by several set screws positioned on flat spots filed onto each shaft. The table is leveled so that rotation is around a true vertical axis. This rotation axis is centered on the incoming light beam. Custom mounting plates are machined so that the sensors may be mounted vertically to rotate in a horizontal plane with the center of the sensor or diffuser, as the case may be, stationary in the beam, i.e., the center of the sensor is on the same axis as the rotation axis of the table. This minimizes sensor wander in the beam.

The beam is formed by a 4 m tube made of 15 cm inside diameter polyvinyl chloride (PVC). The inside surface of the tube is painted with a flat black paint. Two baffling fixtures, consisting of four baffles with 10 cm inside diameters, are positioned within the PVC tube. The beam terminates in the center of a box that contains the table and measures 1.22 × 1.22 × 0.91 m. The box is painted with a very black, fiber-impregnated paint, and black velvet cloth is hung on the walls to further reduce stray light inside the box. The light source consists of a 300-watt, 2.54 cm aperture, axial parabolic confocal xenon arc lamp manufactured by ILC Corporation. This produces an irradiance level of about 200 W/m^2. The total distance between detector and source is 4.5 m. The working aperture is 5 cm with a measured uniformity of about 1%. Except for very large sensors or diffusers, work takes place very near the center of this working aperture.

The table position, sampling interval, sampling dwell time, and number of scans is controlled by a microprocessor-based data acquisition system. This same data logger controls the operation of the rotating shadowband radiometer and is described in Harrison *et al.* (1994). In addition to controlling the operation of the cosine bench, the data acquisition system logs the samples from as many as 16 sensors at each sample position.

A slot that is cut in the rotating platform passes through an optical switch to define the home position approximately 95° from normal incidence. Note that a Lambertian receiver only responds to light incident between 0° and 90°. Dark measurements are made in this position and subtracted from each reading. The dark measurements produce the same values whether the light source is on or off indicating that scattered light within the housing is extremely low. The stepping motor moves the table 0.0625° per step. The table is positioned at 90° incidence angle by stepping from the home position and checking the alignment with a long straight tube mounted on the face of the detector

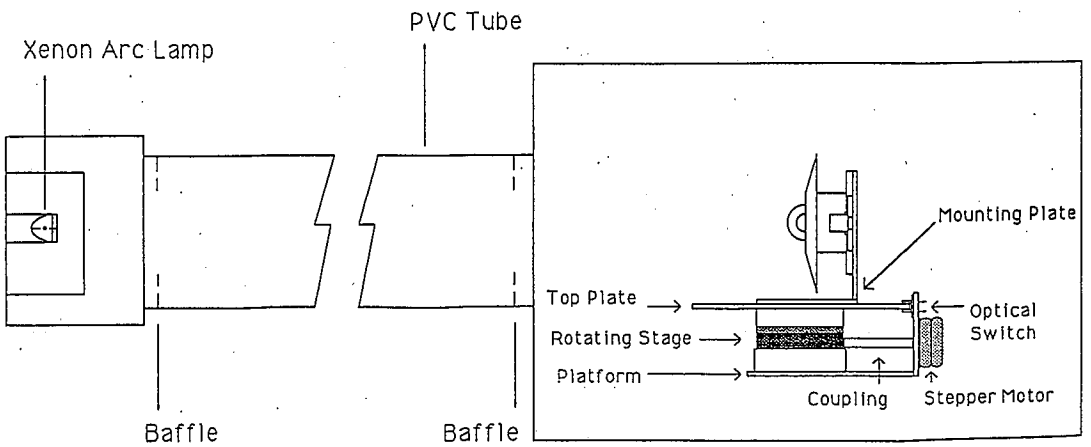

Fig. 2. Schematic layout of cosine response test bench.

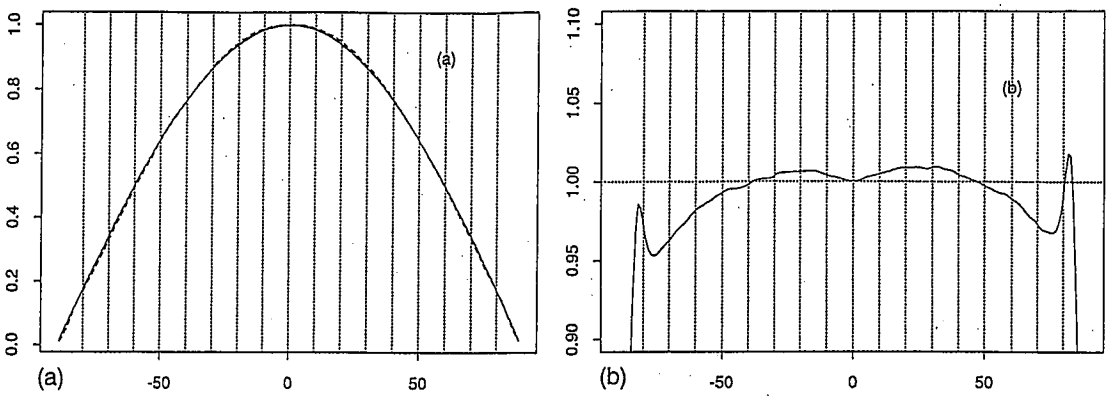

Fig. 3. (a) Ideal and unnormalized cosine responses of silicon cell pyranometer. Note apparent close agreement. (b) Normalized cosine response of silicon cell pyranometer. Note the amplification of differences.

or diffuser. This usually allows alignment to within one step.

A single cosine response scan includes sampling from −90° to +90° and back to −90°. Four scans are made in a typical measurement. More than one scan and sampling in each direction are required to average the small, but inevitable fluctuations in the xenon arc lamp output, even though the power supply provides a constant current to the lamp. Samples are permitted with a resolution as fine as every 0.25°, but more typically are made at 1° intervals. The time spent at each position depends on the response time of the sensor. Silicon cell radiometers and photometers are sampled one second after positioning at each angle, but the longer response time of thermopile radiometers requires a pause of 30 s to 1 min before each sample.

3. COSINE RESPONSE MEASUREMENTS (COMMERCIAL SENSORS)

Some manufacturers of irradiance and illuminance sensors plot the cosine response of their instruments unnormalized. Figure 3(a) illustrates one such plot. A perfect cosine response is represented by the solid line. The measured response of a LI-COR LI-200 pyranometer (1985) is plotted as the dashed line. Plotted in this fashion, the cosine response of the instrument looks remarkably close to perfect. Figure 3(b), on the other hand, illustrates the response on a normalized plot (the way LI-COR illustrates their cosine response). This shows directly the bias one would have for a beam incident from a given direction. For example, one would underestimate the irradiance for a beam incident at −75° by about 5% if corrections were not applied.

Measurements were made of the cosine response characteristics of a number of commercial sensors. Both irradiance and illuminance sensors were tested. In all of the figures that follow, the ratio of the measured cosine response to a true cosine response is plotted. Note that the scale is the same for each instrument tested for easier comparison and that the expansion of the scale, compared to a zero-to-one vertical scale, makes discrepancies readily apparent.

Figures 4(a), 4(b), and 4(c) contain the measured cosine responses of three individual LI-COR LI-200 pyranometers, three individual LI-210 photometers, and two individual LI-190 photosynthetically active radiation sensors. These are three similar instruments with different filtering. They follow the same basic design of Kerr *et al.* (1967) for silicon cell sensors with a silicon cell beneath a diffuser and optical filter as appropriate. The diffuser, which is raised to compensate for the light lost from specular reflection at the top of the diffuser, is surrounded by a shading ring that cuts the light off at 90° incidence angle. Each instrument shows some asymmetry about normal incidence. If the optical axis of the sensor is not exactly perpendicular to the top of the shading ring, which is used for the alignment within the light beam, this asymmetry is expected. The angular misalignment error, θ_{err}, between the actual optical axis of the instrument and the mechanical axis can be estimated by the first moment of the measured angular irradiance function, $I(\theta)$,

$$\theta_{err} = \frac{\int I(\theta)\theta d(\theta)}{\int I(\theta) d(\theta)} \qquad (1)$$

This estimator for the angular error is the maximum-likelihood estimator given uncorrelated, normally distributed residuals. After calculating this factor, the sensor position was adjusted by this angle (to the nearest 0.0625°), the cosine response measurement rerun, and nearly perfect symmetry obtained; thus, verifying that this factor fairly represents the asymmetry. The picture emerges, as we shall see, to show some measurable asymmetry with nearly every instrument. However, in each of these cases, this misalignment of optical and mechanical axes is less than 0.6°. Note that the average shape of the LI-COR instrument response corresponds closely to LI-COR's published cosine response (1985).

Figure 5 is the normalized cosine response from three Eppley Precision Spectral Pyranometers (PSPs)

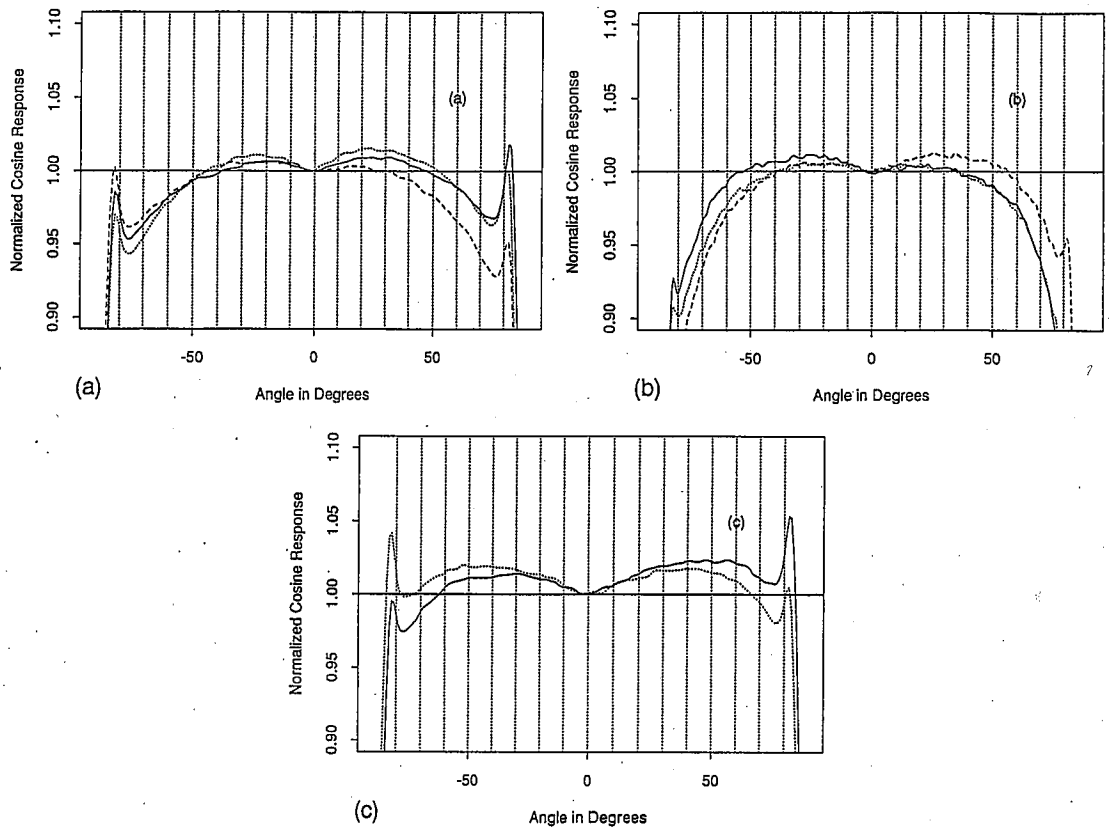

Fig. 4. (a) Normalized cosine responses of three different LI-COR pyranometers. (b) Three different LI-COR photometers. (c) Two different LI-COR quantum sensors.

(1991). Again we note the asymmetry, which in every case is less than 0.5°. The alignment in the light beam in this case was made with the alignment tube on the ring that surrounds the double dome structure. This may explain the asymmetry because this may not be parallel to the detector face, however, this surface would normally be used by us to align the PSP instrument for use outdoors. For the three PSPs tested, the cosine responses show remarkable reproducibility.

The cosine response was measured for the Kipp and Zonen CM 11 (1991). This is a thermopile instrument similar to the Eppley PSP. Its asymmetry is less than 0.6°. Again, the alignment is relative to the flat metal support surrounding the dome. Its cosine response is somewhat better than the Eppley PSPs in that the CM 11's response is closer to one to larger incidence angles (see Fig. 6).

4. COSINE RESPONSE MEASUREMENTS (MFRSR)

The multi-filter rotating shadowband radiometer uses a Kerr *et al.* (1967) type of receiver. The system is described fully in Harrison *et al.* (1994). The MFRSR measures global and diffuse spectral irradi-

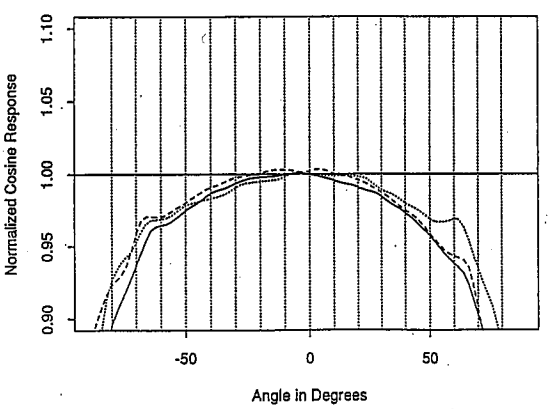

Fig. 5. Normalized cosine responses of three different Eppley PSP pyranometers.

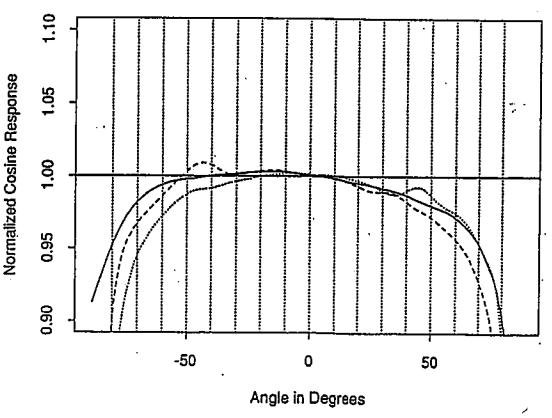

Fig. 6. Normalized cosine responses of three different Kipp & Zonen CM 11 pyranometers.

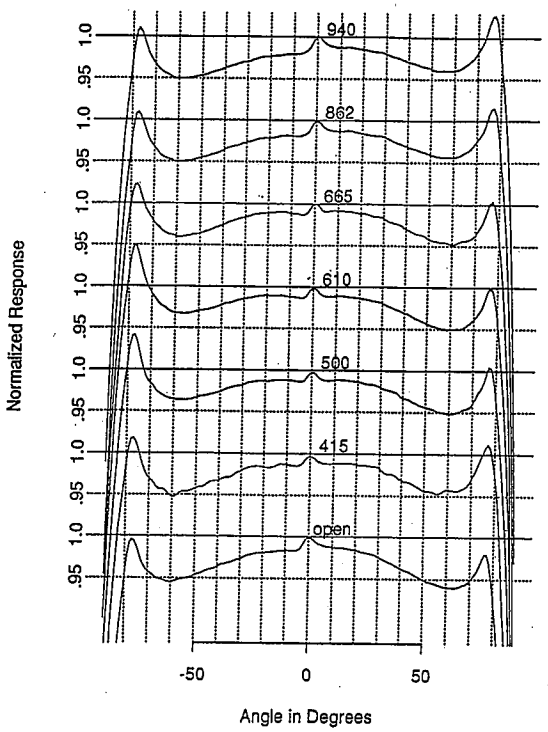

Fig. 7. Normalized cosine responses for seven detectors in the MFRSR detector assembly. "Open" refers to the unfiltered silicon detector and the number labels refer to the central wavelengths of the filters in nanometers.

ances at seven wavelengths by positioning a blocking band out of the field-of-view of the receiver and between the direct solar beam and receiver, respectively. It then calculates direct normal irradiance from these two measurements. All of these irradiance data are obtained simultaneously within a single detector head containing seven filter-detector combinations. The detector head consists of a diffuser and integrating cavity machined from Spectralon (Labsphere, Inc., Sutton, New Hampshire). Two frosted Schott WG-280 glass plates (Schott Glass, Mainz, Germany) act as transmission diffusers to increase the light scattering within the cavity. Radiation exits the bottom of the cavity to irradiate a hexagonal arrangement of six detectors with a seventh detector in the center of this array.

Figure 7 contains seven cosine response plots for the seven sensors of a typical MFRSR head. As one can easily see, the cosine response is slightly different for each position within the MFRSR head. The integrating cavity has eliminated much of the asymmetry. The cosine responses are similar to those in the Fig. 4, which contains responses for other sensors of the Kerr *et al.* (1967) design.

5. CONCLUSIONS

The protocol for all instrument testing was identical. Consequently, this should represent a fair comparison of the cosine response of these instruments. In the cosine bench the light source is a xenon arc lamp. These lamps produce light mainly in the blue and visible and emit poorly in the 1000–2800 nm region and, therefore, are red poor with respect to the sun. Whereas thermopile instruments are presumably insensitive to the wavelength of incident radiation, we cannot rule out the possibility that the optical train may produce some cosine response wavelength dependence.

There was some concern about the stability of the light source even though the current through it is stabilized. Each cosine response curve in Figs. 4–8 is drawn through average values from eight scans at each angle. There is some smoothing before the curves are plotted, but the root-mean-square error of the noise before smoothing is only 0.001. It can be concluded that the light source stability is very good. Otherwise, there would be considerable noise on each response curve from angle to angle as a result of averaging eight time-spaced values.

Silicon cell detectors do not suffer from a "tilt" error, but thermopile sensors may. Nast (1983) tested four thermopile detectors for this effect. He found that the PSP and the CM11 did not show any significant differences when used at an angle different from horizontal alignment. Consequently, all of the silicon cell and thermopile instruments in this paper are free of tilt error.

A point to stress is the importance of automating these tests. Usually the manual testing of instrument cosine response is slow, tedious and only a few angles are measured. For each detector using one degree resolution and four scans, each consisting of measurements beginning at −90° scanning to +90° and then back to −90°, there are 22,912 samples taken, because each sample of a scan is itself an average of 16 rapid samples.

This study reported on only those instruments that were accessible and had sensible cosine responses. Some instruments that were tested had such poor cosine responses, that it was elected not to show them so that subtle effects that are stressed in this study would not be lost. Of course, the tests were not exhaustive. Performance for a particular instrument could be better or worse than those shown. A point that bears repeating is that it was decided to greatly expand the scale at which these plots usually appear to make the points about asymmetry and reproducibility.

All of the detectors tested had angular misalignment errors between the optical and mechanical axes ranging between 0.1° and 0.6°. Despite this small difference, the asymmetry is quite apparent on the plots. These axes misalignments are clearly larger than the error associated with alignment on the cosine bench. How well one can align in the laboratory may be assessed by considering Fig. 8. Figure 8(a) is the cosine response of the same instrument measured 10 times by removing the device and remounting and realigning in the same position as carefully as possible. The test was performed by a trainee. The calculated asymmetry from eqn (1) for the 10 trials was 0.27° +/− 0.09°. We may consider 0.09° (or 1.5 times the step size of our stepping motor) the upper limit for alignment error in the laboratory. Most instruments

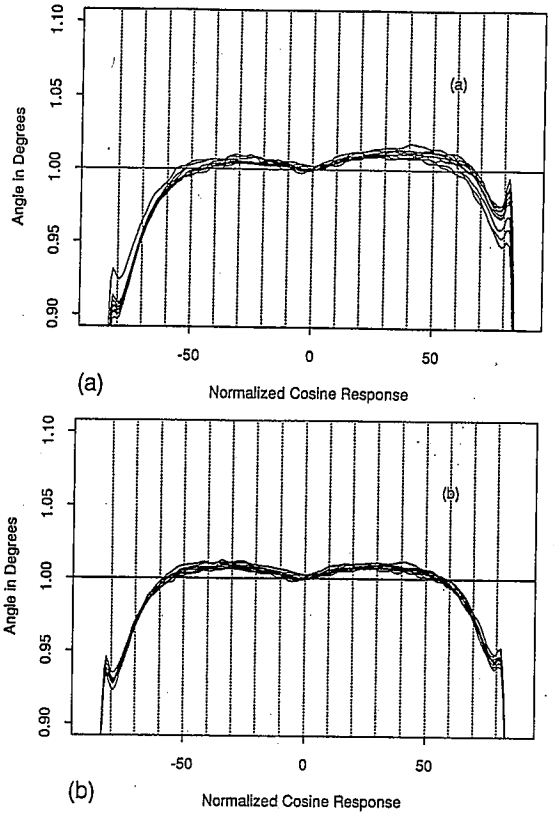

Fig. 8. (a) Ten repeated measurements of cosine response of same sensor to estimate operator ability to reposition sensor in testbed. This allows a bias estimate from misalignment. (b) Mathematically aligned cosine response measurements of (a) to estimate random error in measurement.

mounted in the field are probably aligned less accurately than this.

Errors in the 0.1–0.6° range can be very important to a measurement error budget when high accuracy is desired. For instance, 0.25° in hour angle corresponds to 1 min of time. Therefore, errors in calculating the direct beam component from shaded and unshaded pyranometers may be appreciable, especially at low solar elevations. The error term also affects global horizontal irradiances when the direct beam dominates. In contrast, the diffuse sky irradiances are less affected. For the artificial case of a uniform sky irradiance and a zero surface albedo, the error is sin θ_{err}, where an error of 0.25° in alignment causes an error of 0.5%, less, but not negligible.

The error that one makes using the bench that may be assigned to random error, rather than the bias that we introduce in aligning the instrument, may be assessed using the same 10 measurements. In Fig. 8(b), the optical and mechanical axis misalignment is mathematically corrected using eqn (1) and overplotted these. Using −45° as a typical point on the plot, a standard deviation of 0.2% is found as the random component of the error associated with a cosine response measurement.

A final point is that instruments used for global horizontal irradiance or illuminance measurements may actually perform well for integrated values. When the cosine response straddles the perfect cosine response, summed irradiation or illumination should average to nearly the correct value. Instruments which have cosine responses that deviate in a monotonic way will produce a bias error that depends on the magnitude of the deviation from true cosine behavior. Because instruments are usually calibrated at zero or near normal incidence angles, the cosine response should not affect calibration. It is, however, crucial that cosine response be understood if one attempts to use these instruments for the calculation of direct irradiance.

Acknowledgments—The authors would like to express their appreciation to Chuan Zhou who made many of the measurements. Brian Taylor was responsible for machining the mechanical components. This research was supported at the ASRC by the U.S. DOE's Atmospheric Radiation Measurements Program through grant number DE-FG02-90ER61072 and the Quantitative Links Program, both within the Office of Health and Environmental Research, and by the New York State Energy Research and Development Authority through contract number 1725-EEED-IEA-92. A major portion of this paper was presented in June, 1992 at the American Solar Energy Society annual meeting in Cocoa Beach, Florida.

REFERENCES

Eppley model PSP precision spectral pyranometer brochure, The Eppley Laboratory, Inc., Newport, RI, USA (1991).

L. Harrison, J. Michalsky, and J. Berndt, Automated multifilter rotating shadow-band radiometer: An instrument for optical depth and radiation measurements, *Appl. Opt.* **33,** 5118–5125 (1994).

J. P. Kerr, G. W. Thurtell, and C. B. Tanner, An integrating pyranometer for climatological observer stations and mesoscale networks, *J. Appl. Meteorol.* **6,** 688–694 (1967).

Kipp & Zonen pyranometer (solarimeter)-CM 11 brochure, Kipp & Zonen, Delft, Holland (1991).

LI-200SZ pyranometer sensor instruction manual, LI-CAR, Inc., Lincoln, NE, USA (1985).

P.-M. Nast, Measurements of the accuracy of pyranometers, *Solar Energy* **31,** 279–282 (1983).

R. Philipona, A. Heimo, and B. Hoegger, Investigations of solar radiation detectors using a laboratory test facility for solar radiation meteorological instruments, *Solar Energy* **51,** 159–163 (1993).

M. R. Riches, T. L. Stoffel, and C. V. Wells, *International energy agency conference on pyranometer measurements,* Solar Energy Research Institute Report SERI/TR-642-1156, Golden, CO, USA (August 1982).